Supporting Information

Facile rhodamine-based colorimetric sensors for sequential detections of Cu (II) ion and pyrophosphate ($P_2O_7^{4-}$) anion

Reguram Arumugaperumal,[a] Venkatesan Srinivasadesikan,[b] Ming-Chang Lin,[b] Muthaiah Shellaiah,[a] Tarun Shukla[a] and Hong-Cheu Lin[a]*

[a]*Department of Materials Science and Engineering, National Chiao Tung University, Hsinchu 300, Taiwan.*
[b]*Center for Interdisciplinary Molecular Science, Department of Applied Chemistry, National Chiao Tung University, Hsinchu 300, Taiwan.*
linhc@mail.nctu.edu.tw

Contents

Synthesis of compound (1**)**

A 1.0 M solution of BBr_3 in 20 mL (20 mmol) of CH_2Cl_2 was added drop wise through a septum with use of a syringe to a stirred solution of 1gm (5.2 mmol) 1,2- dimethoxy-3,6-diformylbenzene in 10mL of dry CH_2Cl_2 at –78 ºC. The reaction mixture was stirred under inert atmosphere for an additional 30 min at room temperature. The reaction mixture was subsequently poured into 100 mL of ice water, stirred for 30min, and then saturated with NaCl salt. The product was isolated by extraction into 100 mL of CH_2Cl_2 three times, washed with H_2O, dried in Na_2SO_4, and evaporated to afford 2,3-dihydroxyterephthalaldehyde (**1**) as a grassy yellow solid (780 mg, 90%). ^{1} H-NMR (DMSO-D_6) δ :10.74 (2H, b, OH), 10.30 (2H, s, CHO), 7.26 (2H, s, aromatic CH); ^{13} C-NMR (DMSO-D_6) δ: 193.0, 151.2, 126.1, 119.1.

Synthesis of compound (2)

To a solution of salicylaldehyde (1.5 g, 2.25 mmol) and bis(2-chloroethyl) ether (0.85 g, 6 mmol) in DMSO (20 mL), were added NaOH (360 mg, 9 mmol). The suspension was heated at 120 ºC for 24 h. After cooling the reaction mixture was subsequently poured into 100 mL of water and extracted with CH_2Cl_2followed by a saturated aqueous solution of sodium chloride was added. The water layer was combined and reextracted with CH_2Cl_2. The combined organic layers were dried over anhydrous $MgSO_4$, concentrated *in vacuo* and the crude product was purified by column chromatography EA:hexane (1:9, v/v) The product was obtained as a pale yellow solid; yield 1.13 g, 59 %; ^{1}H NMR ($CDCl_3$) δ: 10.48 (s, 2H), 7.78 (dd, 2H, J = 6.9 Hz and 1.8 Hz), 7.54 - 7.48 (m, 2H), 7.04 – 6.96 (m, 4 H), 4.25 (t, 4H, *J* = 6 Hz), 3.97 (t, 4H, *J* = 6 Hz) ppm. ^{13}C NMR ($CDCl_3$) δ: 189.6, 161.0, 135.9, 128.4, 125.0, 121.1, 112.8, 69.90, 68.3.

Synthesis of compound (3)

To a 100 mL flask, rhodamine B (2.4 g, 5 mmol) was dissolved in 50 mL ethanol. 6.0 mL (excess) hydrazine hydrate (85%) was then added drop wise with vigorous stirring at room temperature. After the addition, the stirred mixture was heated to reflux in an air bath for 2 h. The solution changed from dark purple to light orange and became clear. Then reaction mixture was cooled and solvent was removed under reduced pressure. 1 M HCl (about 100 mL) was added to the solid in the flask to generate a clear red solution. After that, 1 M NaOH (about 150 mL) was added slowly with stirring until the pH of the solution reached 9~10. The resulting precipitate was filtered and washed 3 times with 25 mL water. The product was dried in hot air oven for 24 h obtained as a 1.6 g 4 (75%) as

pink solid. ^{1}H NMR (CDCl3) δ: 7.94 (dd, 1H, *J* = 2.4 Hz and 6.3 Hz), 7.46 – 7.43 (m, 2H), 7.11 (dd, 2H, *J* = 3.9 Hz and 4.5 Hz), 6.45 (d, 2H, *J* = 8.7 Hz), 6.41 (d, 2H, *J* = 2.1 Hz), 6.30 (dd, 2H, J = 2.4 Hz and 9 Hz), 3.53 (bs, 2H), 3.36 (q, 8H, J = 6.9 Hz), 1.16 (t, 12H, J = 6.9 Hz); ^{13}C NMR (CDCl3) δ: 166.1, 153.8, 151.5, 148.8, 132.5, 130.0, 128.1, 128.0, 123.8, 122.9, 108.0, 104.6, 98.0, 65.94, 44.4, 12.6.

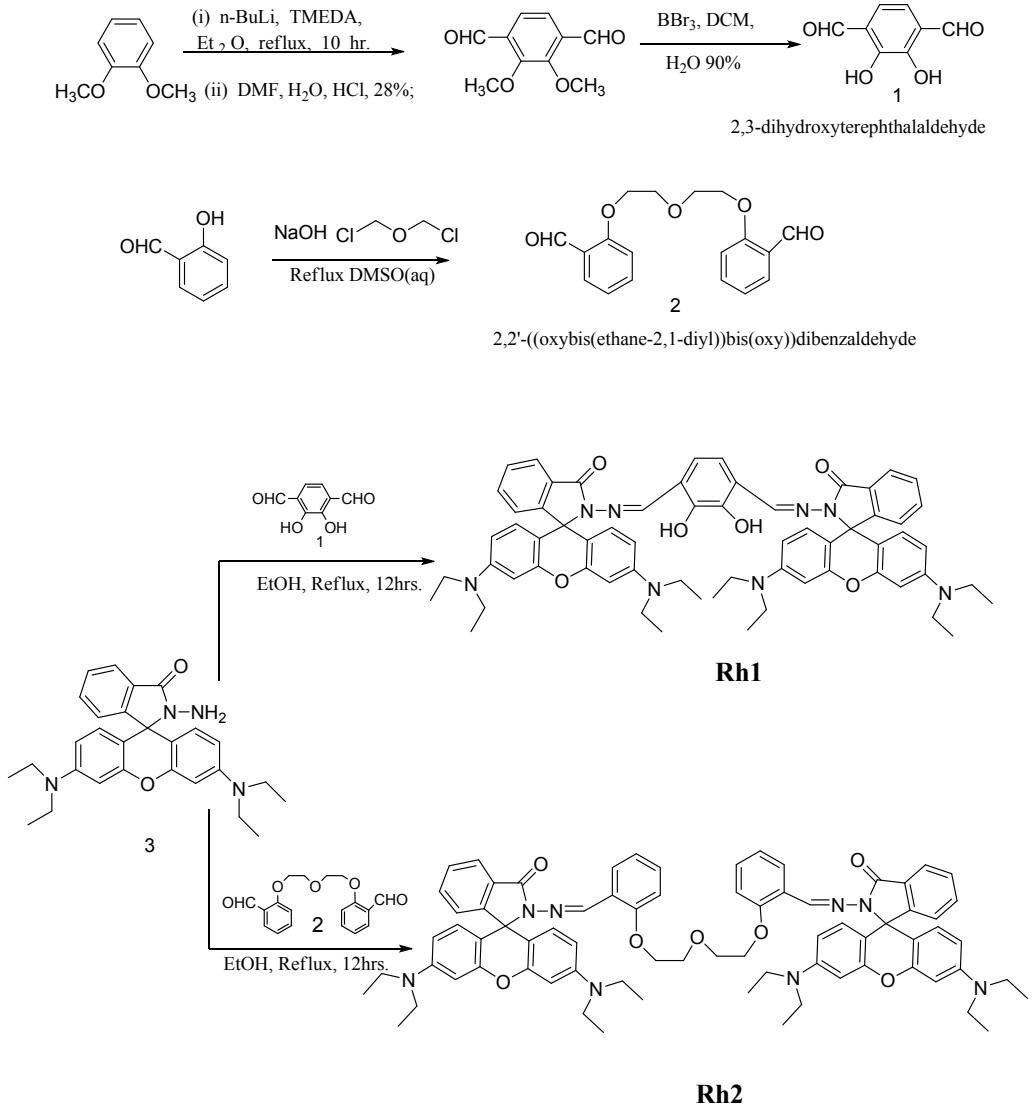

Scheme S1 Synthetic procedures of **Rh1** and **Rh2**.

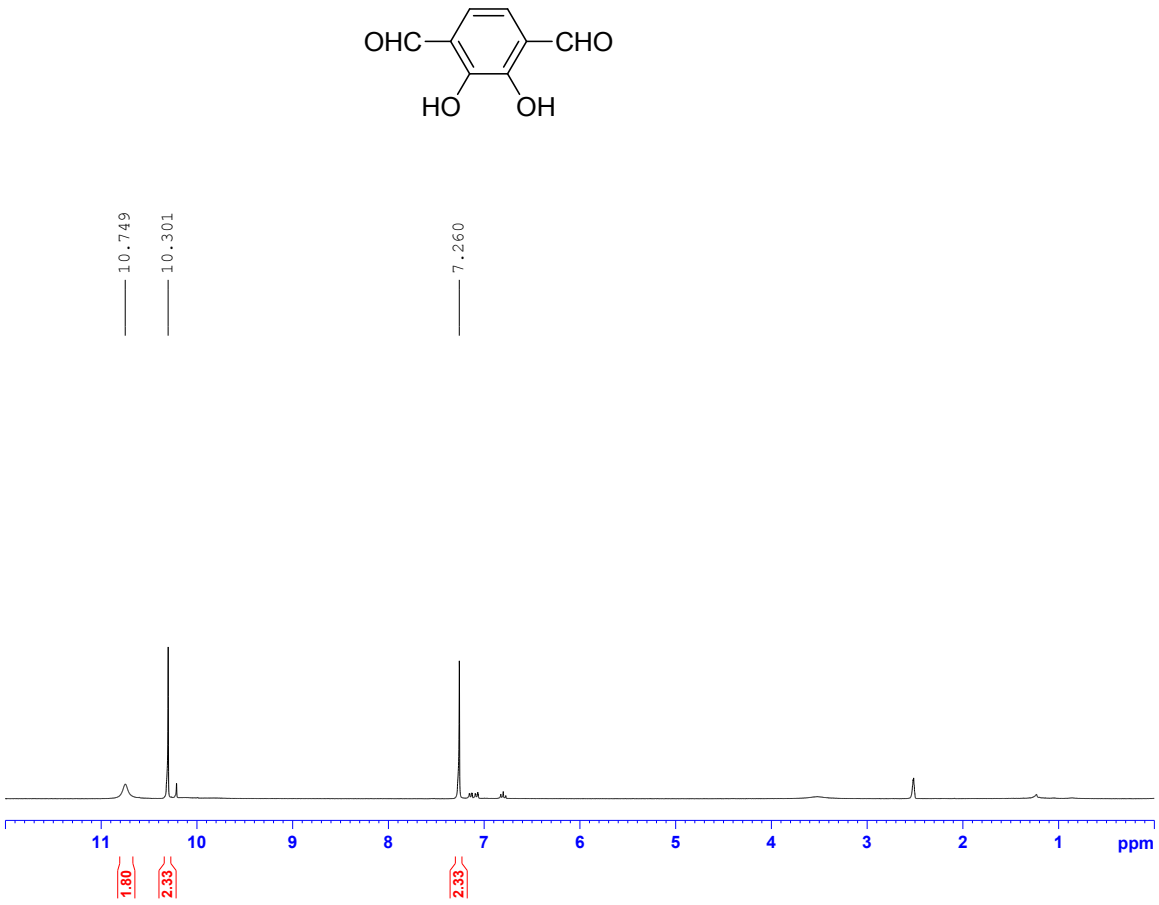

Fig. S1 ^{1}H NMR spectrum of compound **1** in DMSO.

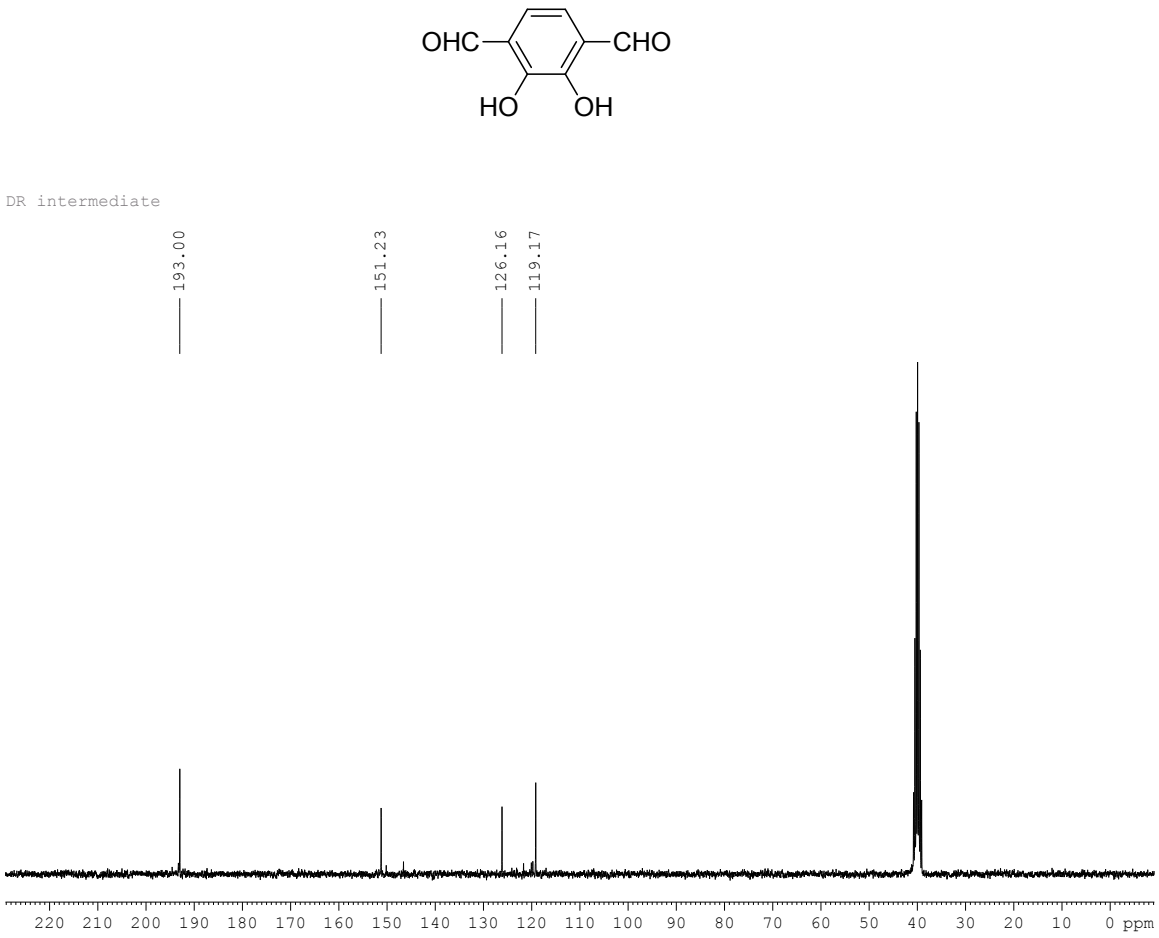

Fig. S2 ^{13}C NMR spectrum of compound **1** in DMSO.

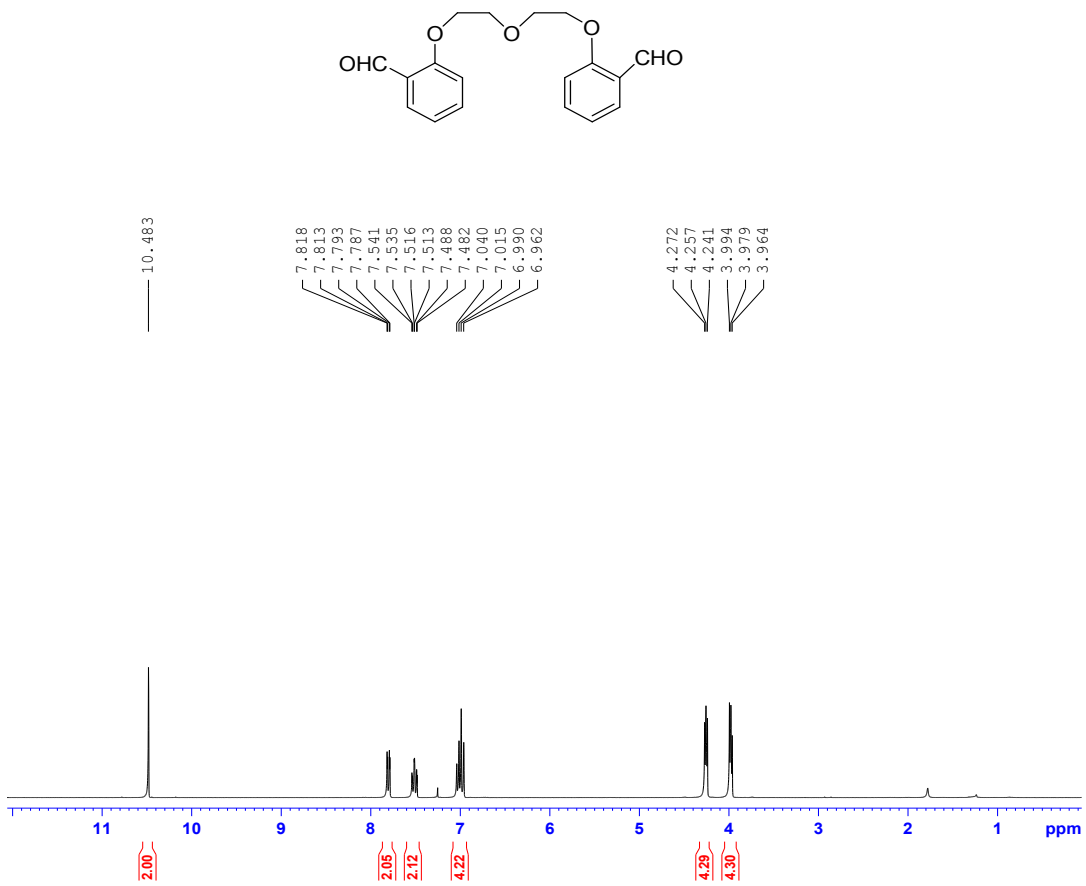

Fig. S3 ^{1}H NMR spectrum of compound **2** in $CDCl_3$.

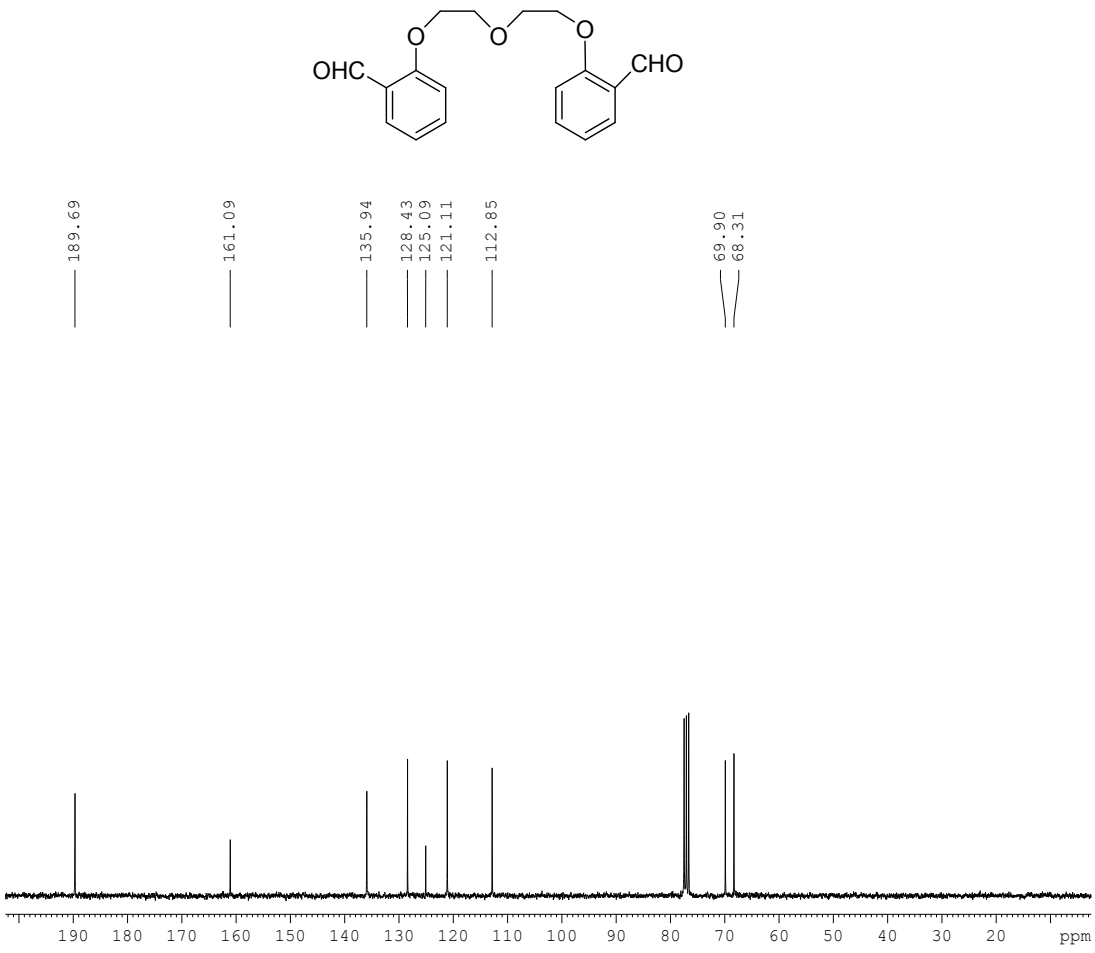

Fig. S4 ^{13}C NMR spectrum of compound **2** in $CDCl_3$.

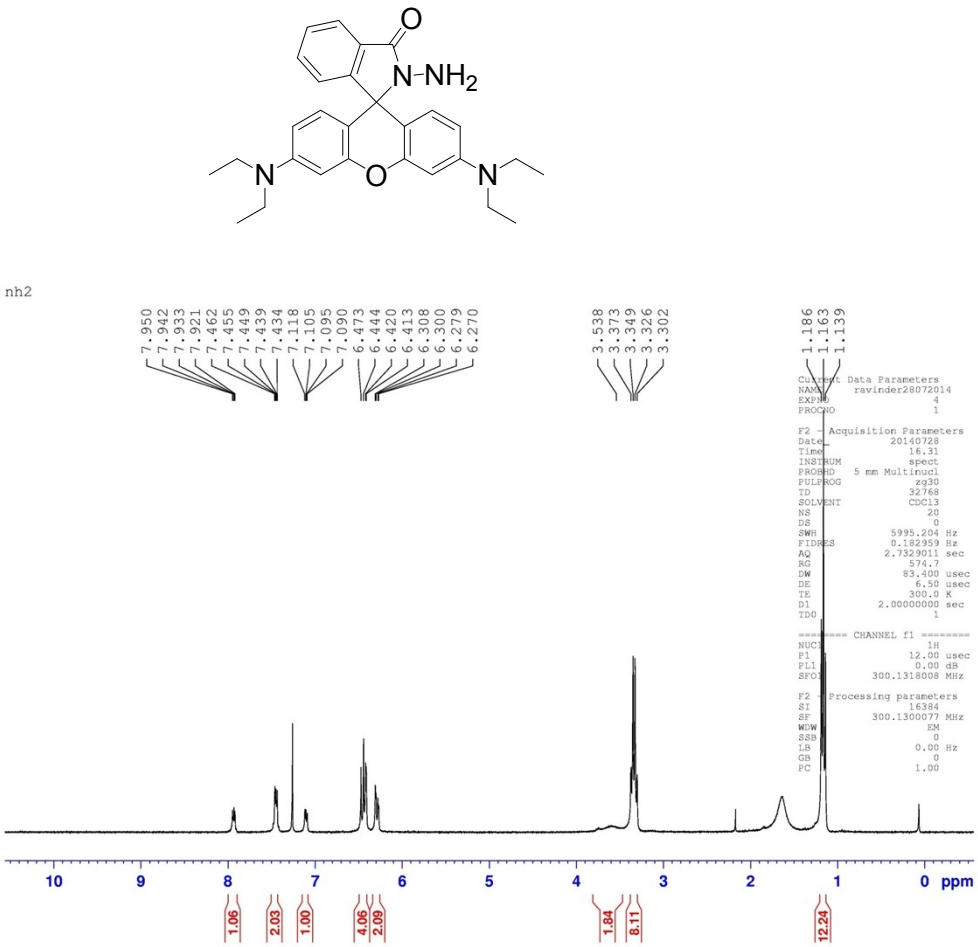

Fig. S5 ^{1}H NMR spectrum of compound **3** in $CDCl_3$.

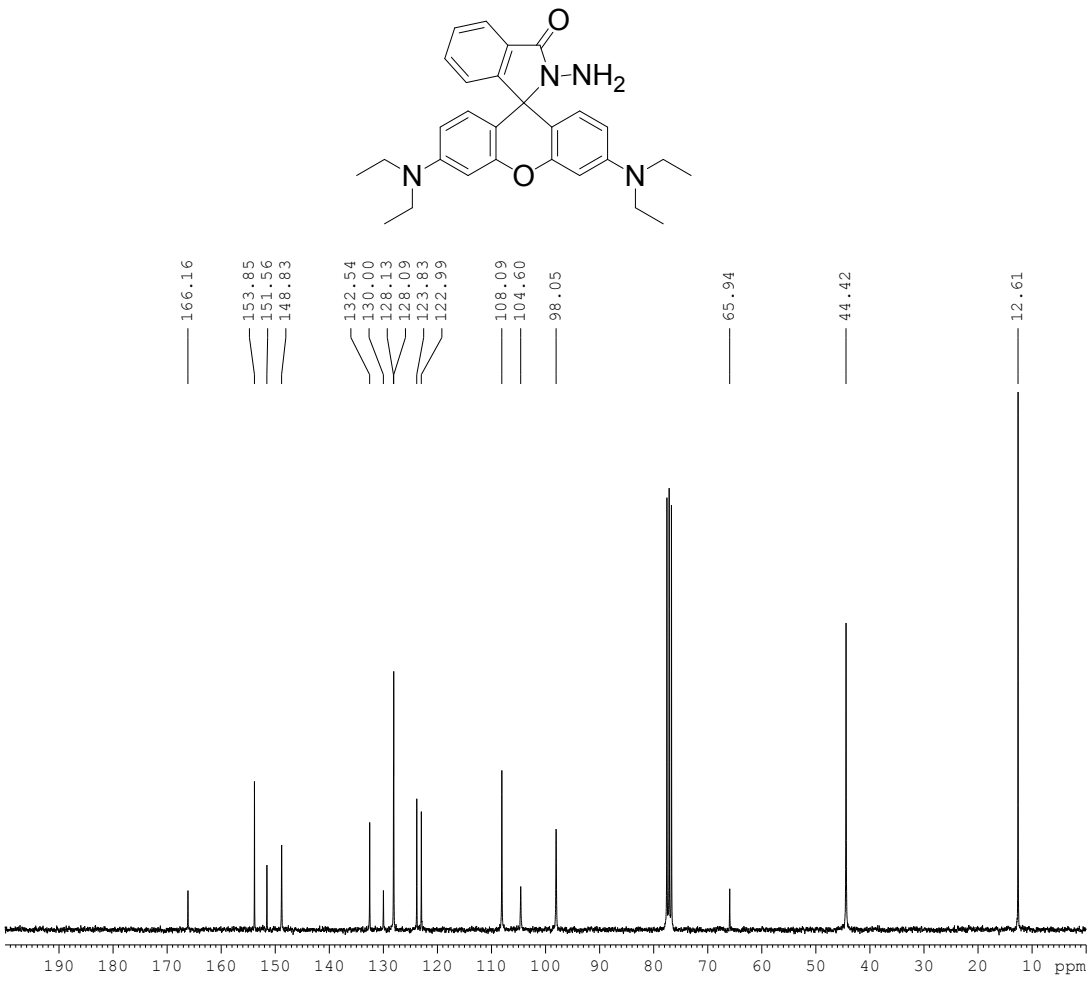

Fig. S6 ^{13}C NMR spectrum of compound **3** in $CDCl_3$.

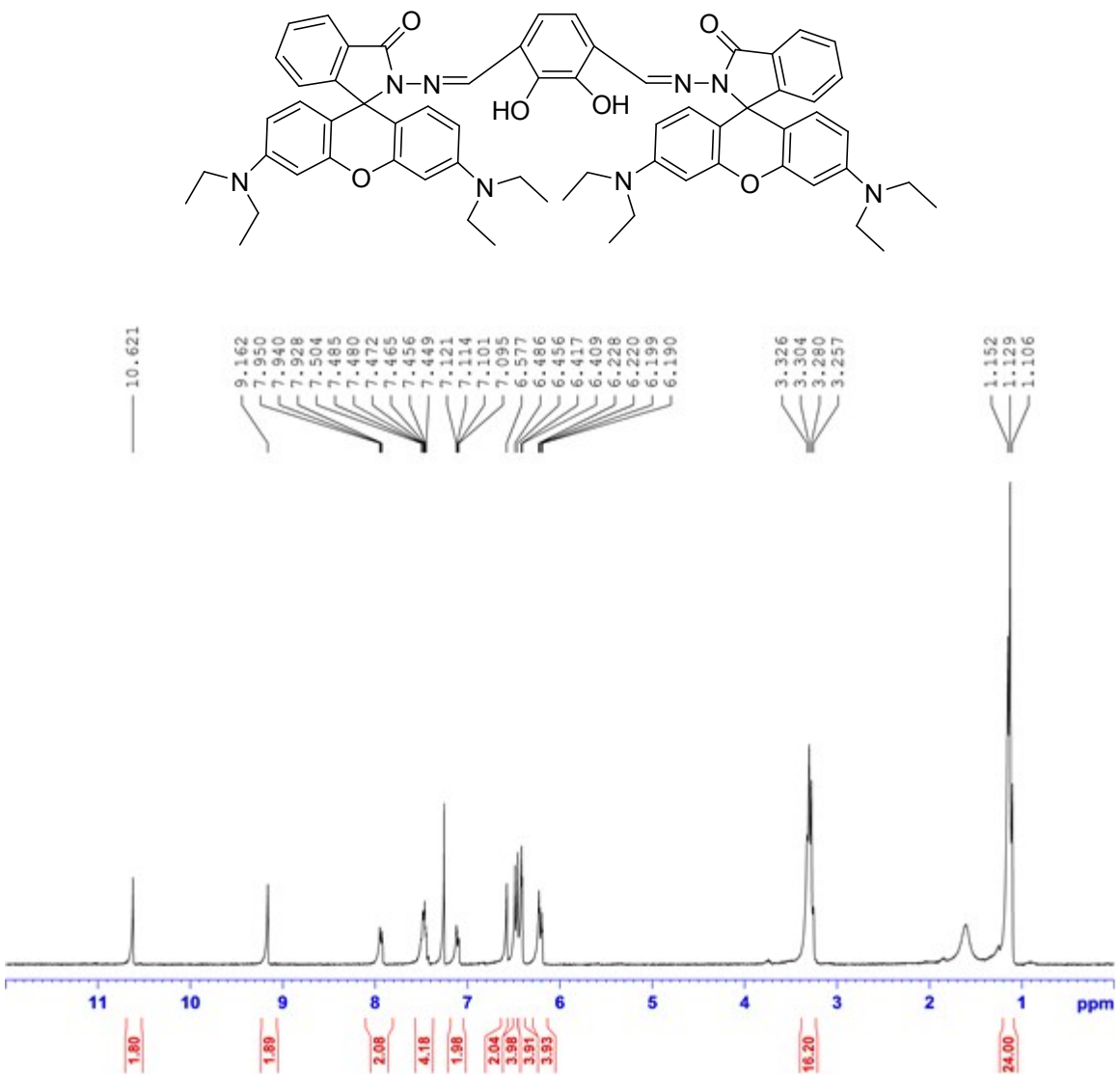

Fig. S7 ^{1}H NMR spectrum of probe **Rh1** in $CDCl_3$.

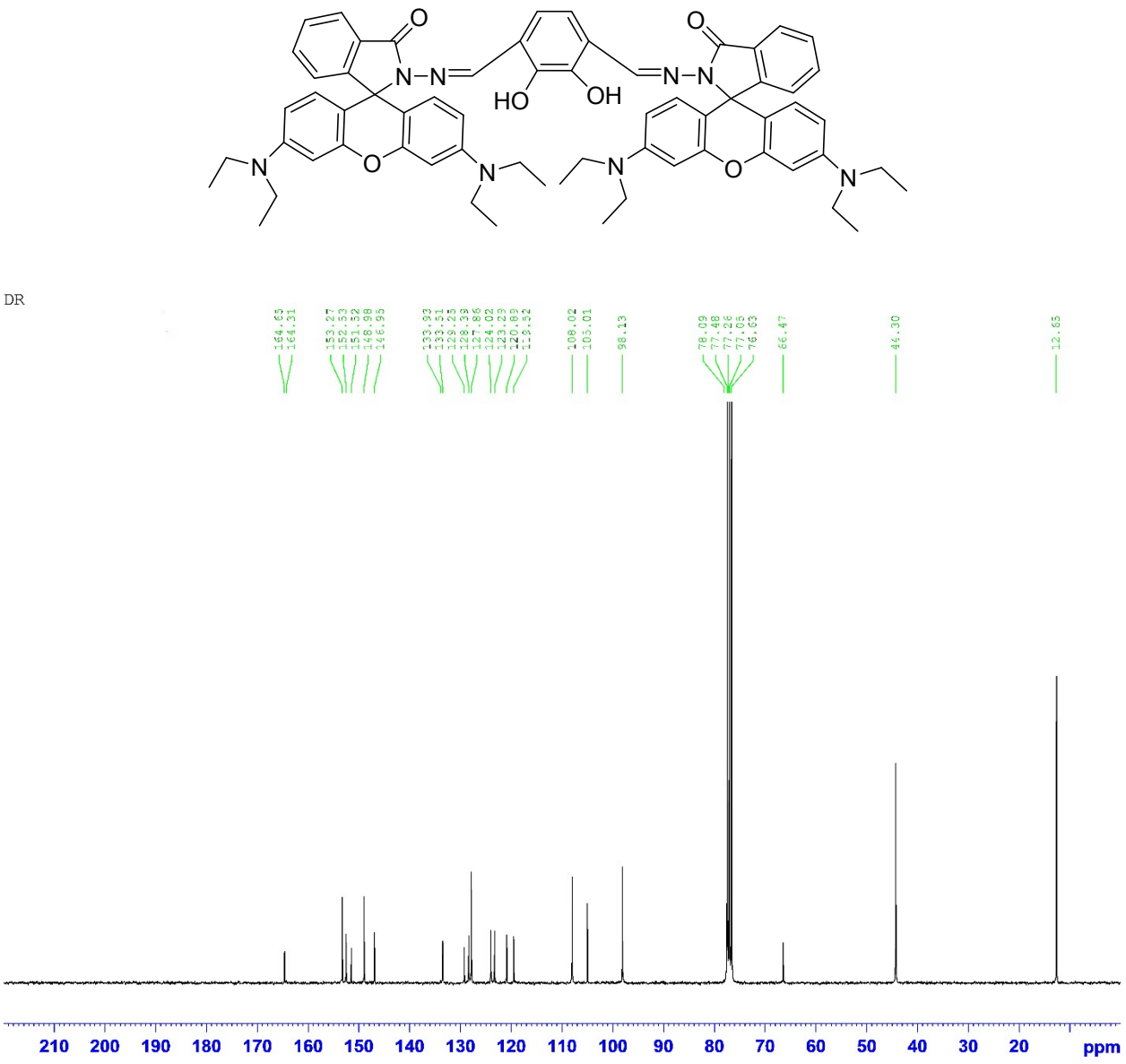

Fig. S8 ^{13}C NMR spectrum of probe **Rh1** in $CDCl_3$.

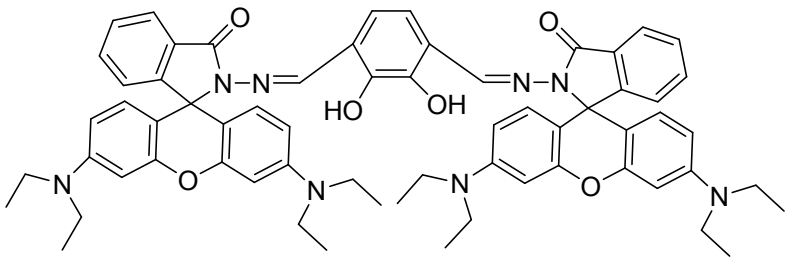

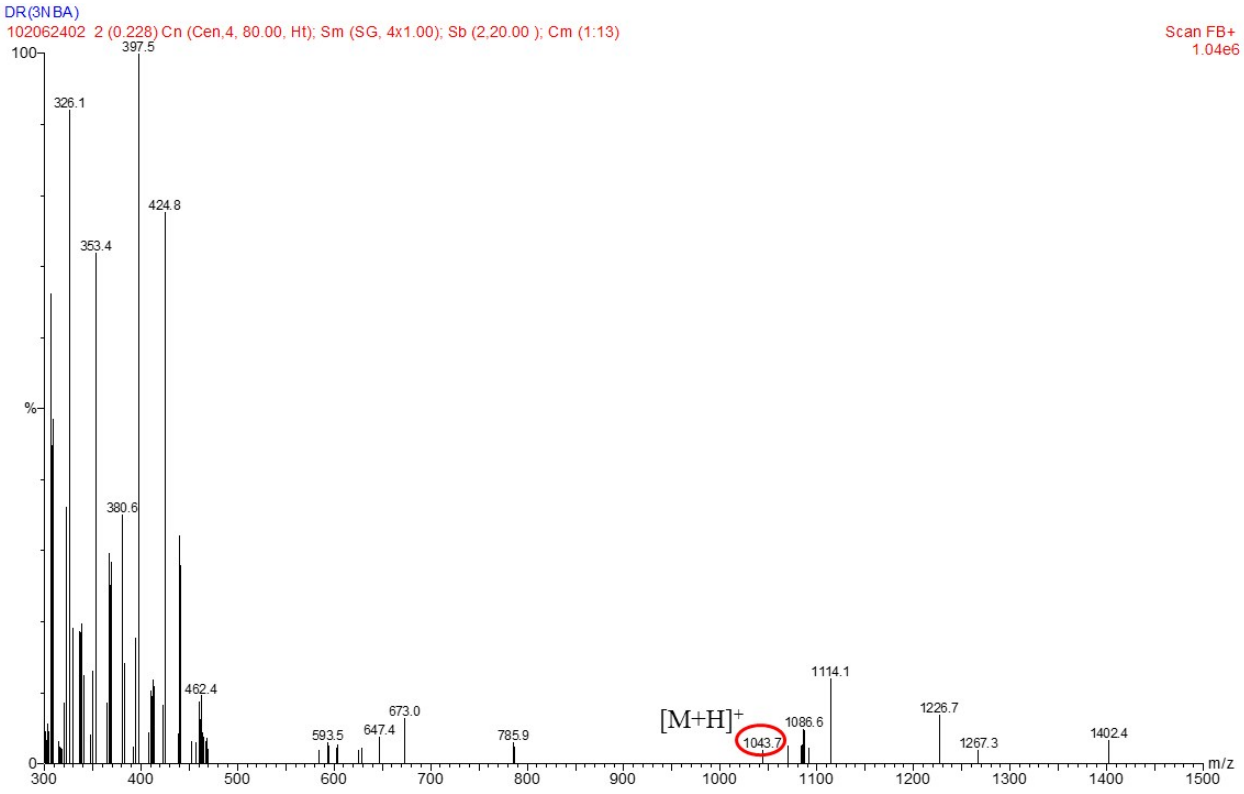

Fig. S9 Mass (FAB) spectrum of probe **Rh1**.

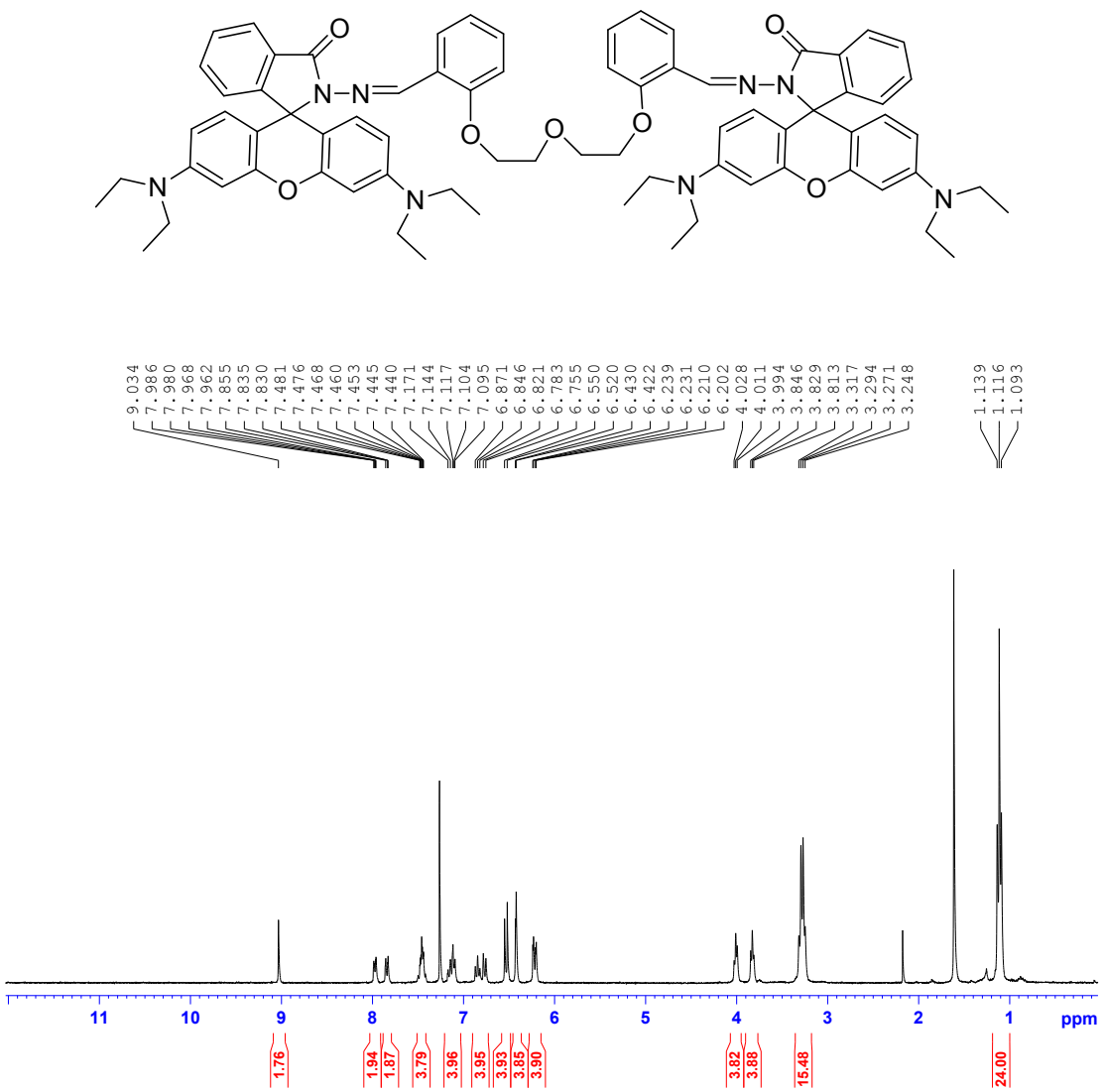

Fig. S10 ^{1}H NMR spectrum of probe **Rh2** in DMSO-d_6.

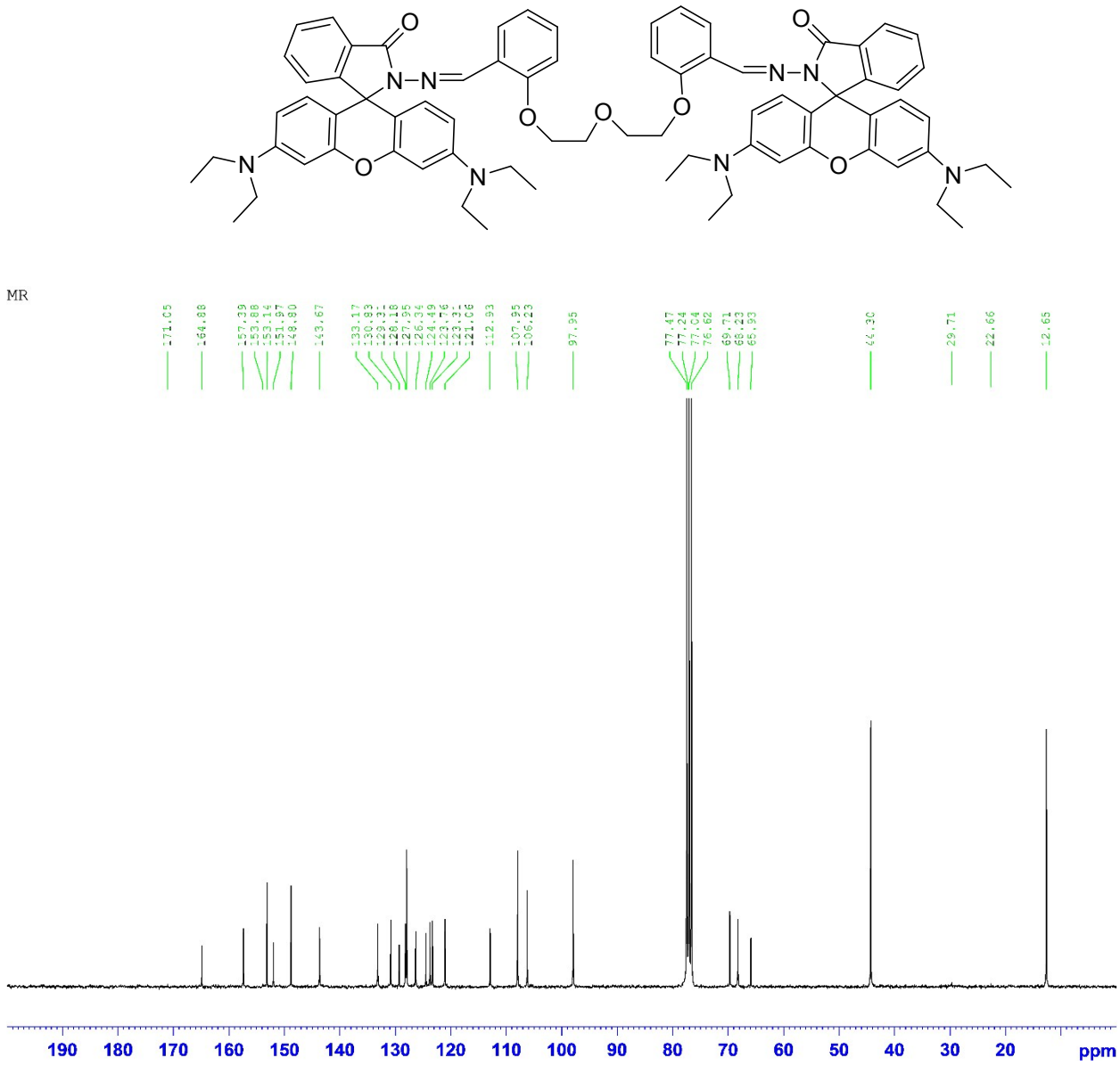

Fig. S11 ^{13}C NMR spectrum of probe **Rh2** in $CDCl_3$.

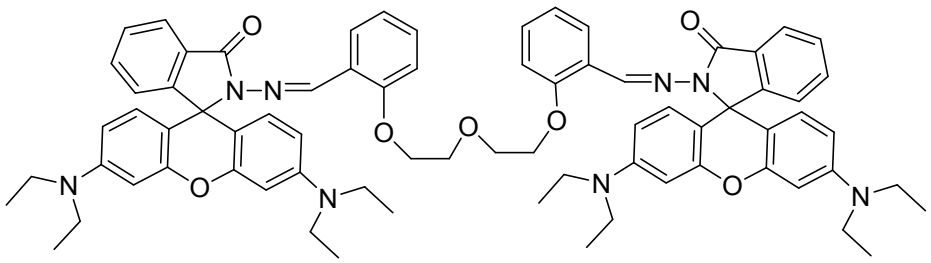

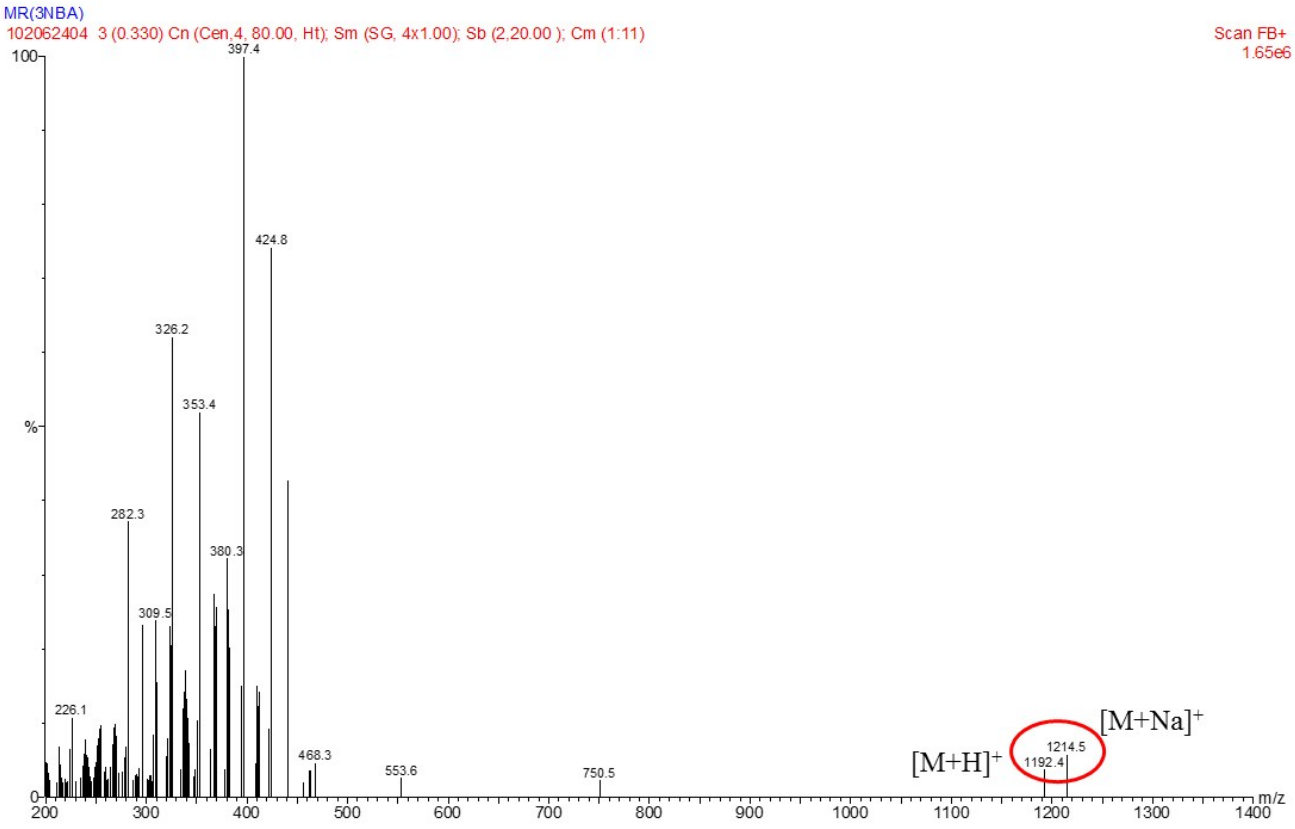

Fig. S12 Mass (FAB) spectrum of probe **Rh2**.

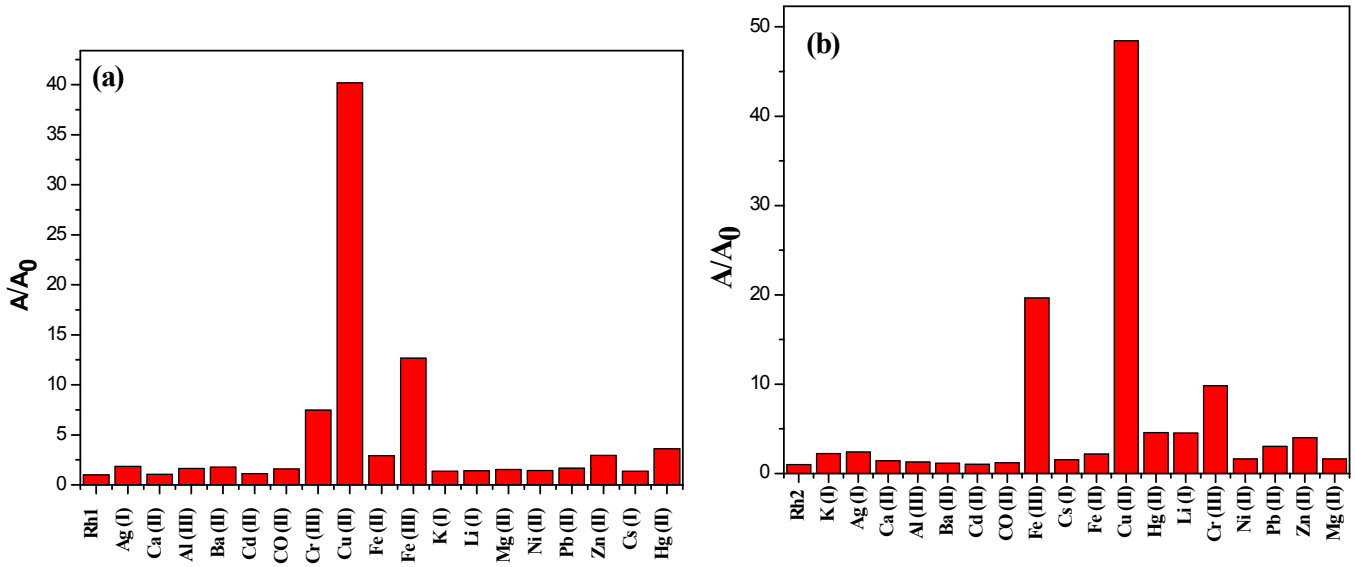

Fig. S13 UV Absorption responses of sensor probes (a) **Rh1** and **(b) Rh2** (10 μM) in $CH_3CN–H_2O$ (v/v = 9 : 1, 5mM Tris-HCl, pH 7.4) in the absence and presence of various metal ions (2.4 and 5 equivs., respectively) absorbance at 554 nm.

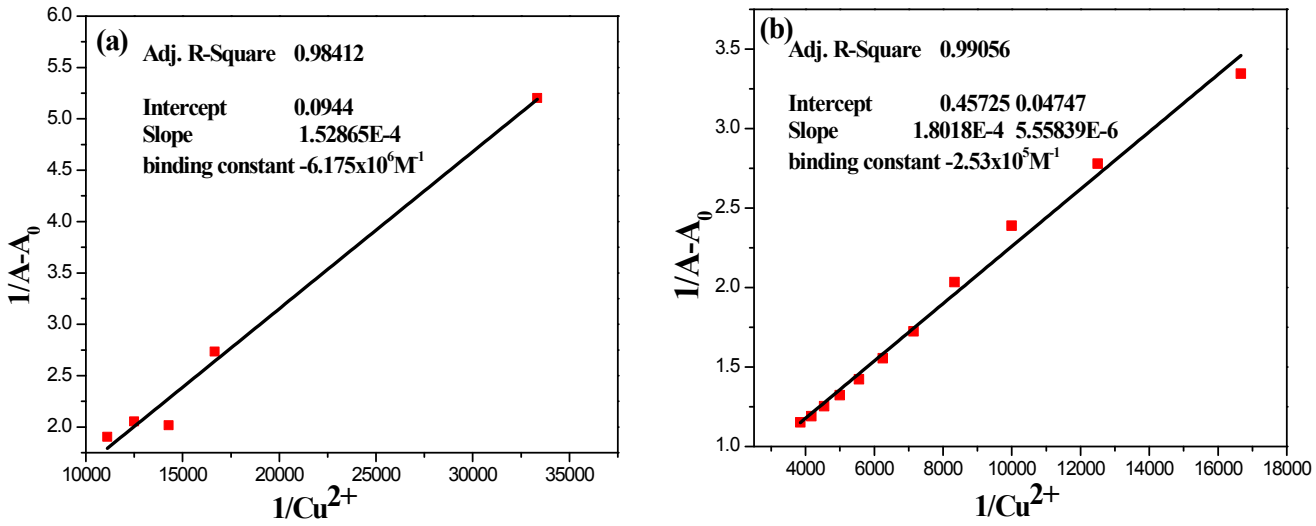

Fig. S14 Binding constants of (a) **Rh1** and (b) **Rh2** for the titration of Cu^{2+} against the ratio of colorimetric response for chemosensor (10 μM) in $CH_3CN–H_2O$ (v/v = 9 : 1, 5mM Tris-HCl, pH 7.4).

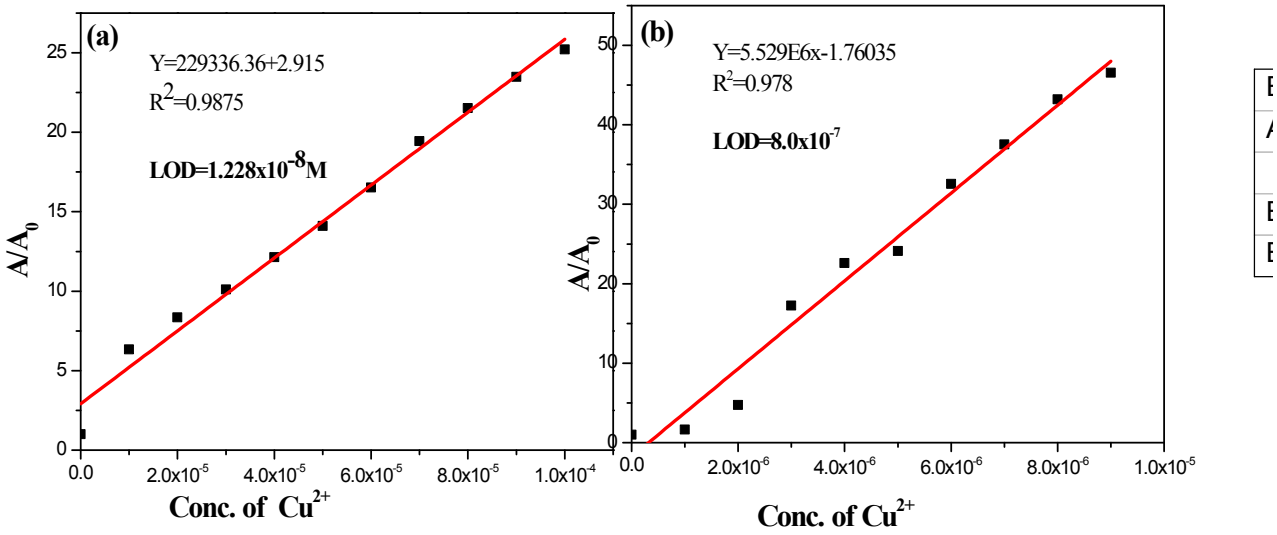

Fig. S15 Standard deviations and linear fit equations for detection limit calculations of (a) **Rh1** and (b) **Rh2**. [Note: Detection limit calculations were based on the absorbance changes versus Cu^{2+} metal ion concentrations.]

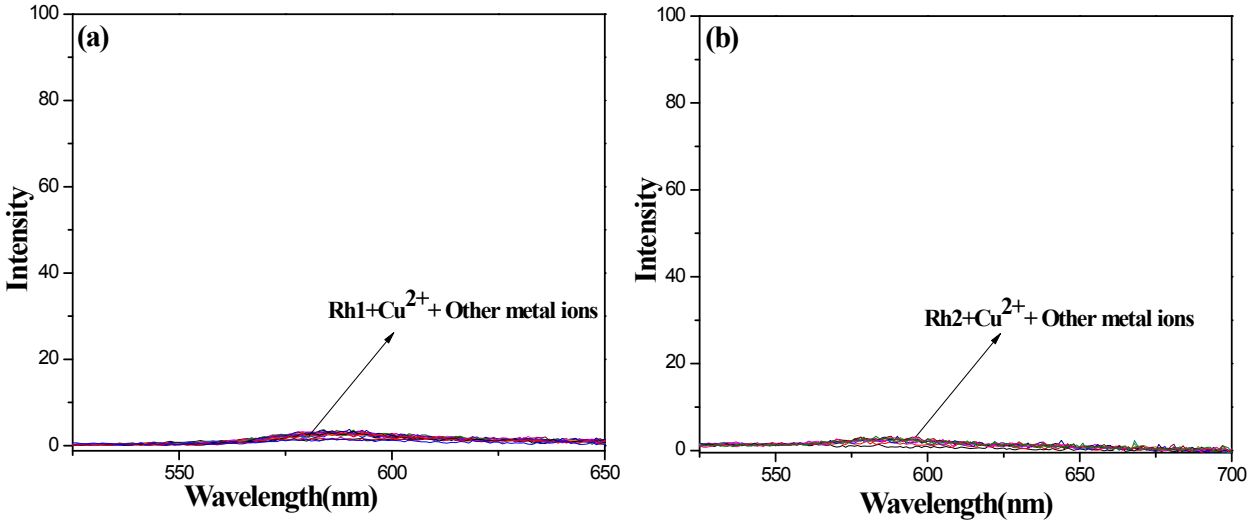

Fig. S16 Fluorescence spectra of (a) **Rh1** and **(b) Rh2** (10 μM) in CH_3CN–H_2O (v/v = 9 : 1, 5mM Tris-HCl, pH 7.4) upon the addition of 5 equiv. metal ions. (Ex. 550 nm)

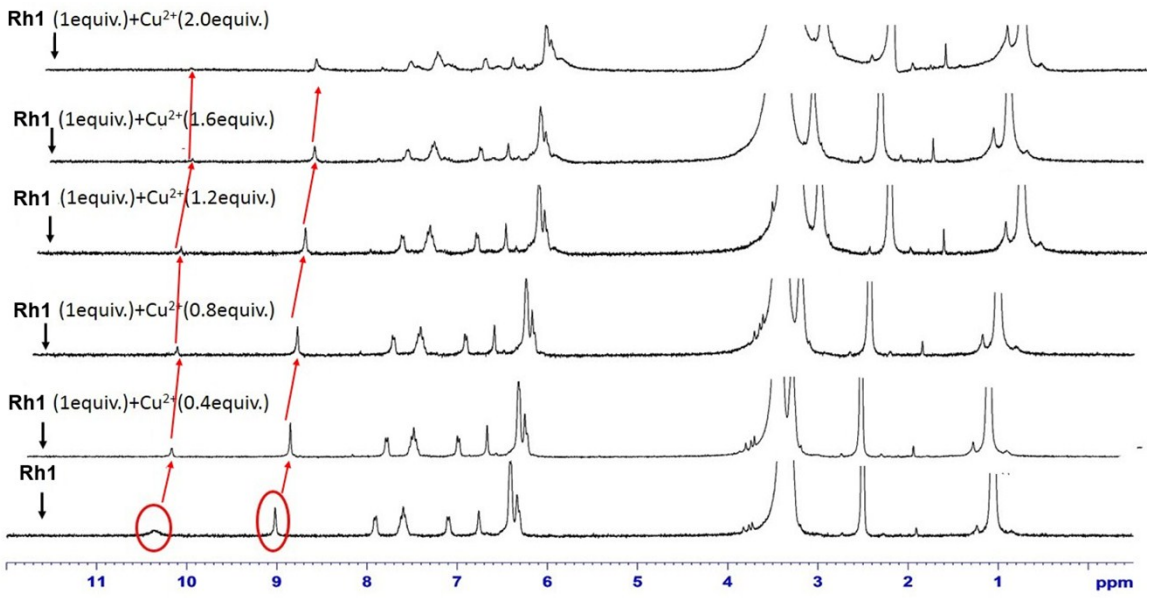

Fig. S17 ^{1}HNMR spectral changes of **Rh1** (10 mM) in DMSO-d_6 titrated with (0–2) equiv. of Cu^{2+} in D_2O.

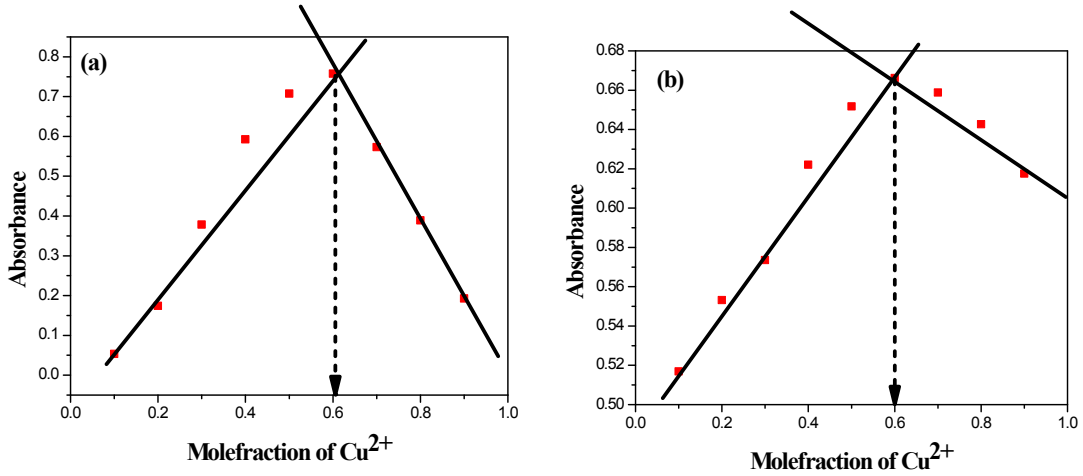

Fig. S18 Job plots according to the method for continuous variations, the total concentration of (a) **Rh1** and (b) **Rh2** (50 μM in CH_3CN–H_2O (v/v = 9 : 1, 5mM Tris-HCl, pH 7.4). The stoichiometries of complexes **Rh1-Cu^{2+}** and **Rh2-Cu^{2+}** were determined according to the method for continuous variations. The absorbance values against the molar ratios of $[Cu^{2+}]/([Cu^{2+}] + [probe])$ show and a feature point between 0.6 abscissa in both **Figs.** (a) and (b) indicating the 1:2 stoichiometry of both complexes **Rh1-Cu^{2+}** and **Rh2-Cu^{2+}**.

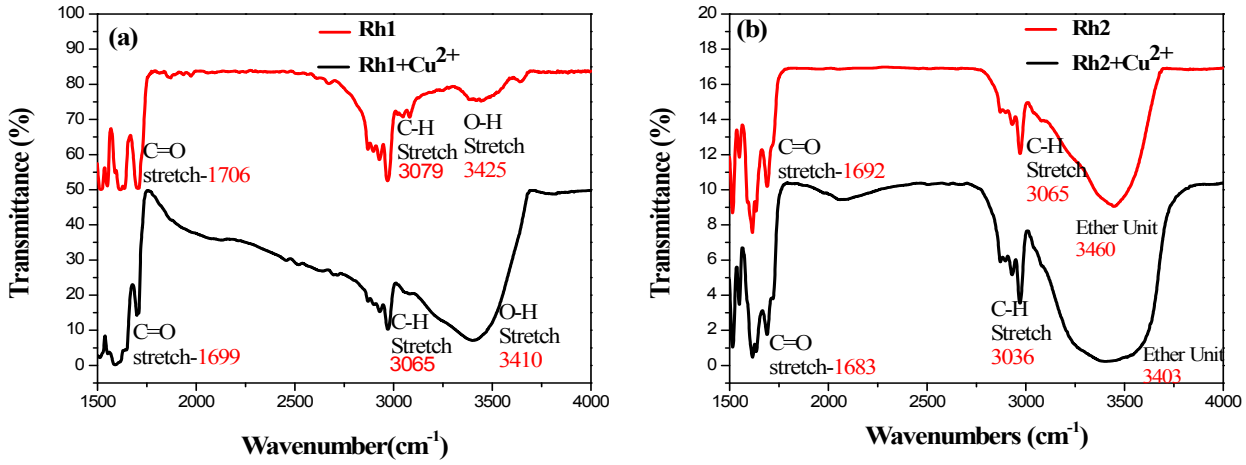

Fig. S19 FT-IR spectra of colorimetric sensor probes (a) **Rh1**, **Rh1-Cu^{2+}** and (b) **Rh2**, **Rh2-Cu^{2+}**.

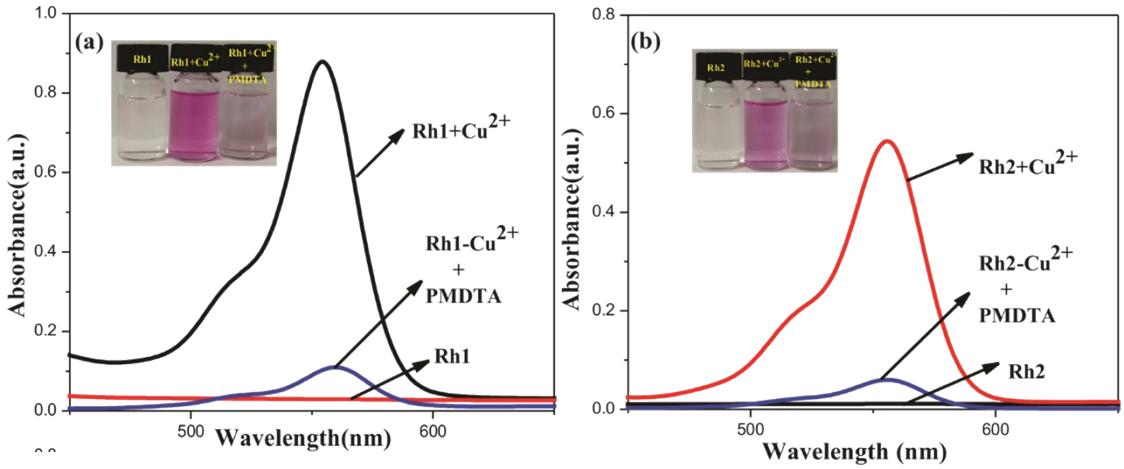

Fig. S20 Reversibility tests of sensor probes (a) **Rh1-Cu^{2+}** and (b) **Rh2-Cu^{2+}**.

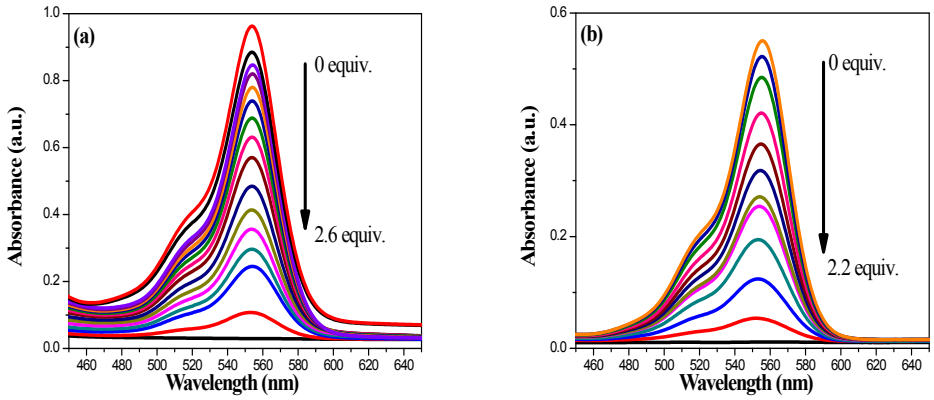

Fig. S21 Reversibilities of (a) **Rh1**-Cu^{2+} and (b) **Rh2**-Cu^{2+} by the addition of PMDTA (0-2.6 equiv. and 0-2.2 equiv., respectively).

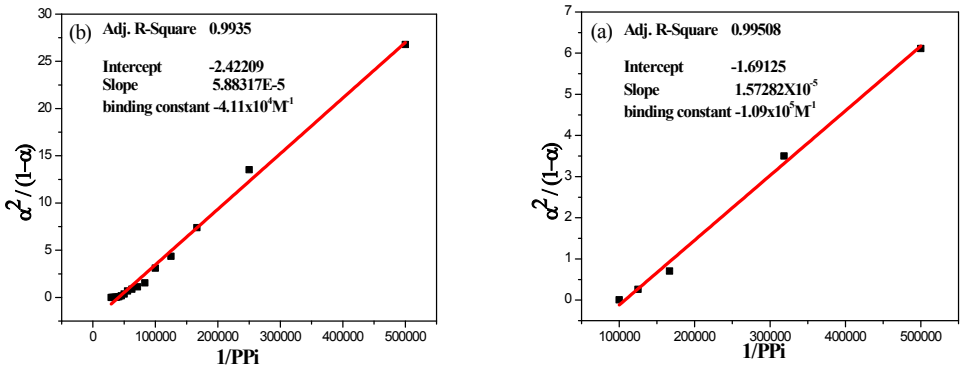

Fig. S22 Binding constants of (a) **Rh1**-Cu^{2+} and (b) **Rh2-** Cu^{2+} for the titration of PPi against the ratio of colorimetric response for chemosensor (10 μM) in $CH_3CN–H_2O$ (v/v = 9 : 1, 5mM Tris-HCl, pH 7.4).

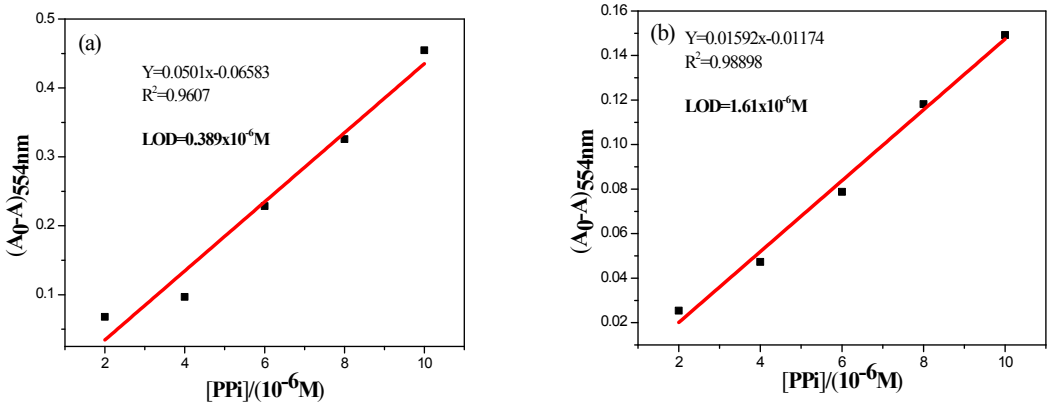

Fig. S23 Standard deviations and linear fit equations for detection limit calculations of (a) **Rh1**-Cu^{2+} and (b) **Rh2**-Cu^{2+}. [Note: Detection limit calculations were based on the absorbance changes versus PPi anion concentrations.]

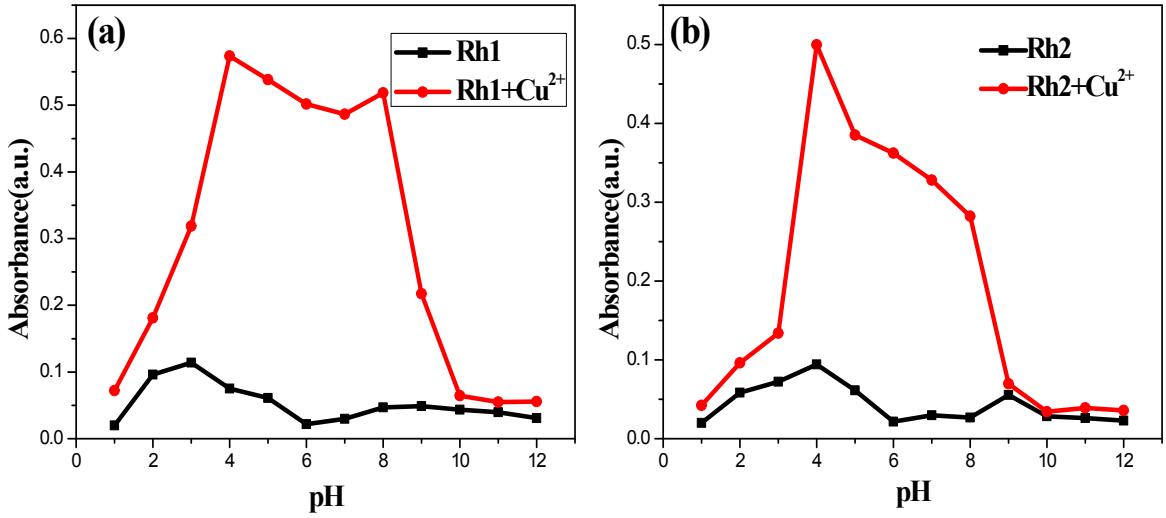

Fig. S24 Absorption intensity of free (a) **Rh1** and (b) **Rh2** (10 μM) in aqueous solution CH_3CN–H_2O (v/v = 9 : 1, 5mM Tris-HCl, pH 7.4) with and without Cu^{2+} ion (2 equiv.) as a function of pH. [Note: Absorption intensity at 554 and 556 nm, respectively.]

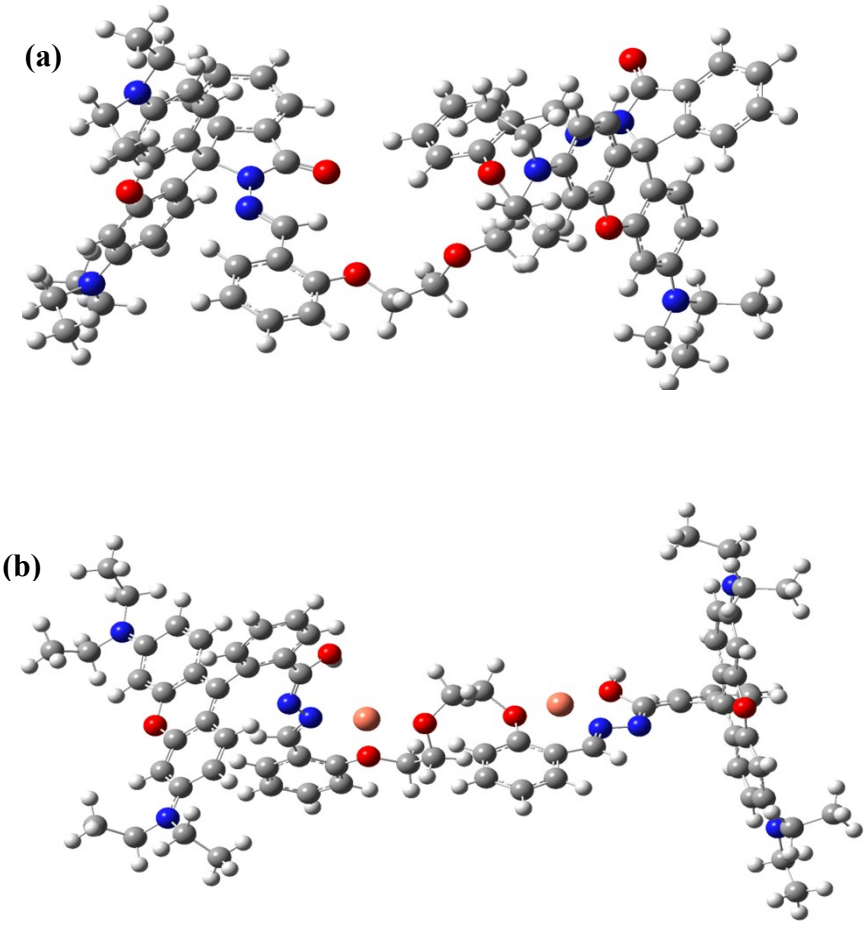

Fig. S25 Optimized structures of (a) **Rh2** and (b) **Rh2-Cu^{2+}** at B3LYP /LANL2DZ level.

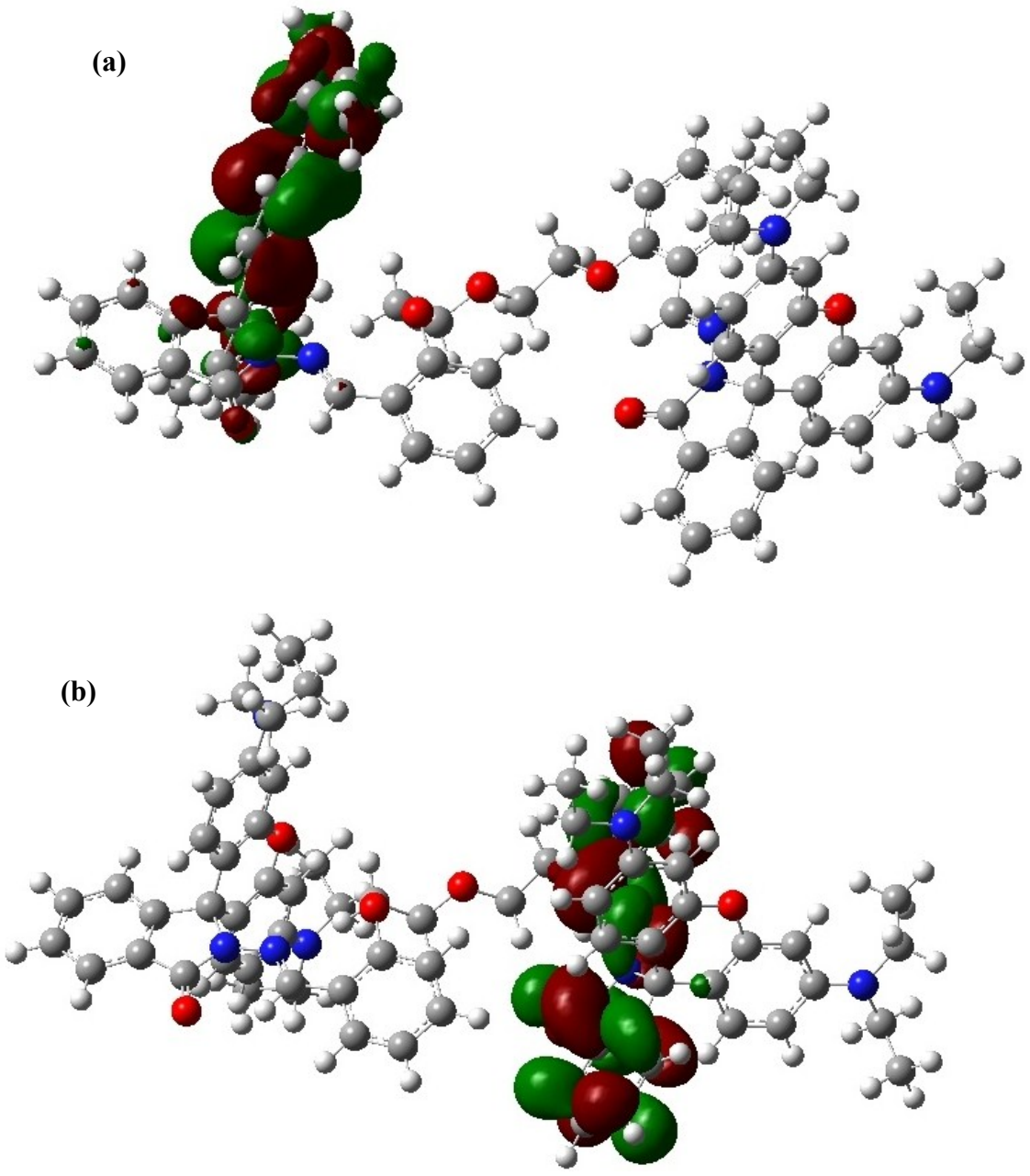

Fig. S26 (a) HOMO and (b) LUMO structures of **Rh2** at B3LYP/LANL2DZ level in the gas phase.

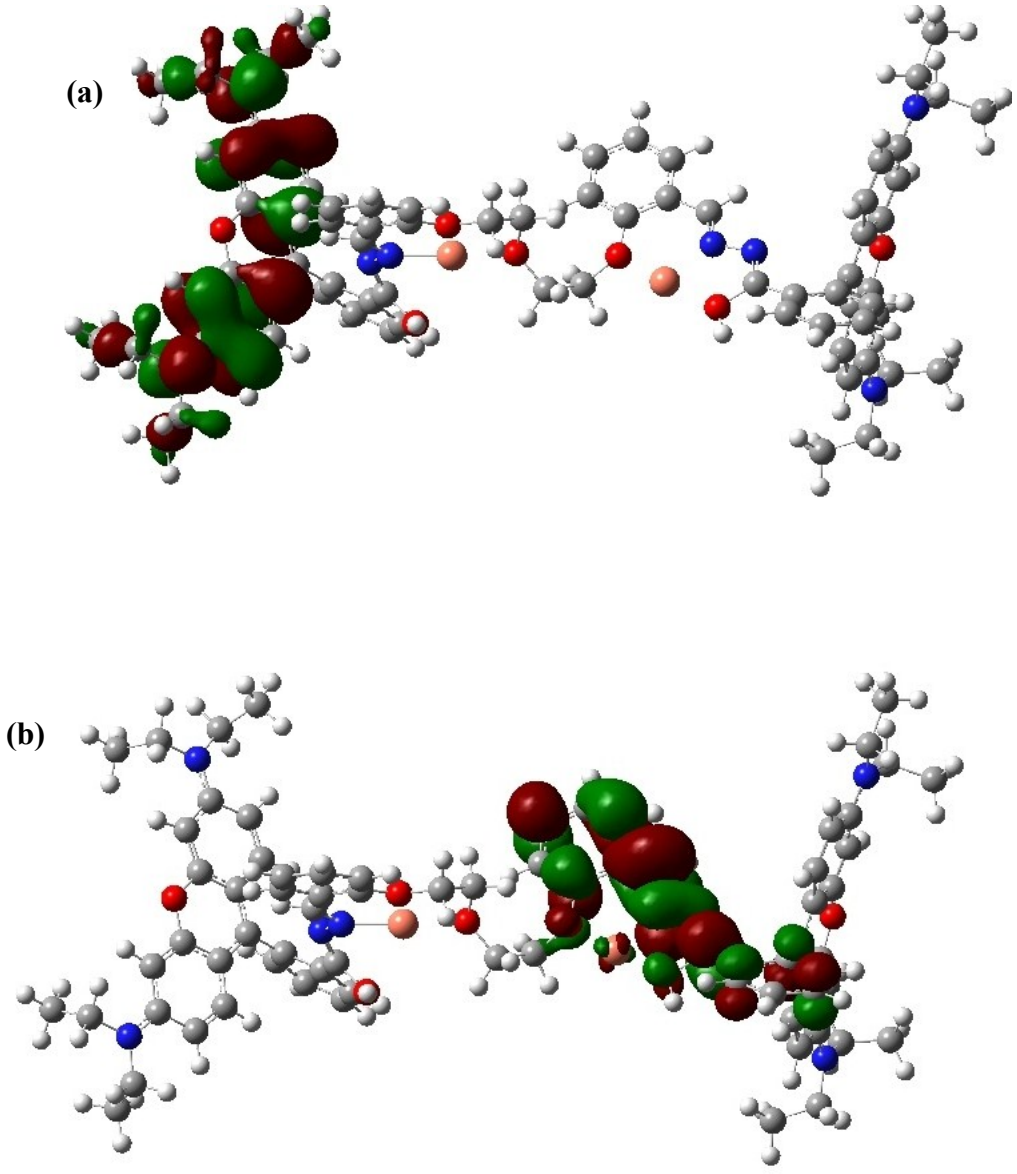

Fig. S27 (a) HOMO and (b) LUMO structures of complex **Rh2-Cu^{2+}** at B3LYP/LANL2DZ level in the gas phase.

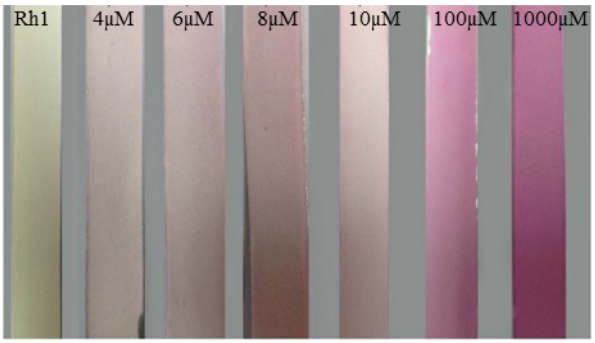

Fig. S28 Photographs of sensor tests on **Rh1** (1 x 10^{-4} M) strips for the detection of Cu^{2+} in aqueous solution with different concentrations. From left to right: **Rh1** (probe), 4, 6, 8, 10, 100 and 1000 μM.

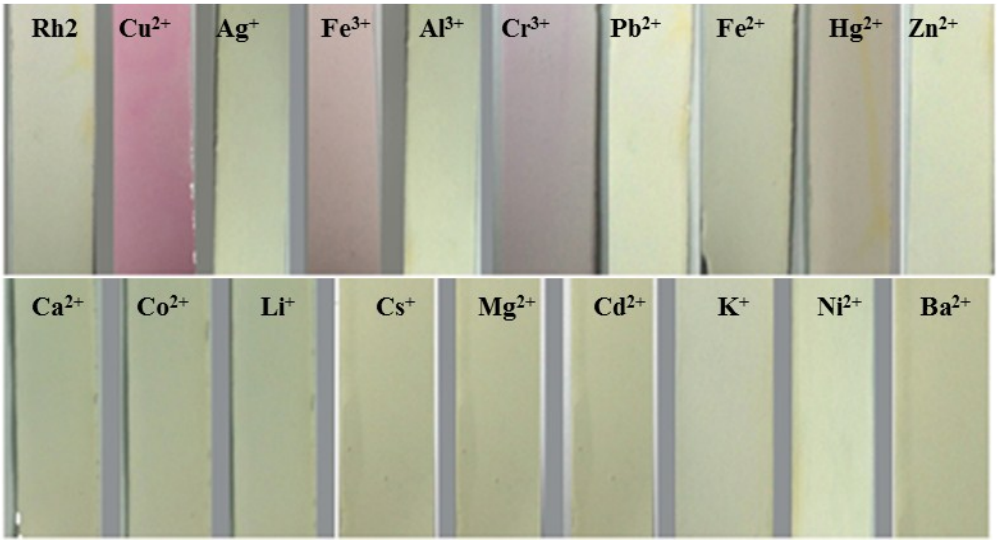

Fig. S29 Photographs of sensor tests on **Rh2** (1 x 10^{-4} M) strips in the presence of various metal ions (1 x 10^{-3} M).

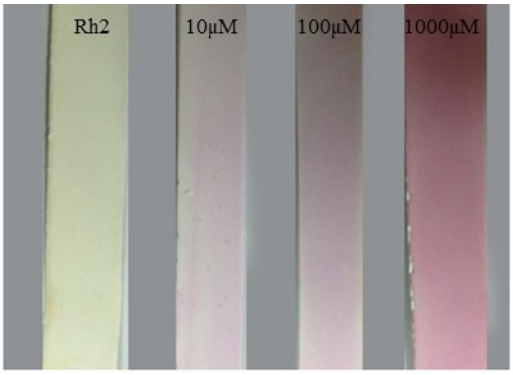

Fig. S30 Photographs of sensor tests on **Rh2** (1 x 10^{-4} M) strips for the detection of Cu^{2+} in aqueous olution with different concentrations. From left to right: **Rh2** (probe), 10 μM, 100 μM and 1000 μM.

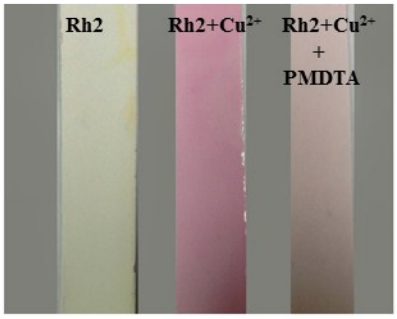

Fig. S31 Photographs of reversibility tests on **Rh2** (1x10^{-4} M) strips in the presence of **PMDTA** (1 x 10^{-5} M). From left to right: **Rh2**, **Rh2-Cu^{2+}** and **Rh2-Cu^{2+}+PMDTA**.